Agricultural and Forest Meteorology 222 (2016) 1–9

Agricultural and Forest Meteorology

journal homepage: www.elsevier.com/locate/agrformet

Observational study on complementary relationship between pan evaporation and actual evapotranspiration and its variation with pan type

Hongchao Zuo[a], Bolong Chen[a,*], Shixin Wang[a], Yang Guo[a], Bin Zuo[a], Liyang Wu[a], Xiaoqing Gao[b]

[a] Key Laboratory for Semi-Arid Climate Change of PRC Ministry of Education, College of Atmospheric Sciences, Lanzhou University, Lanzhou 730000, China
[b] Key Laboratory of Land Surface Process and Climate Change in Cold and Arid Regions, Chinese Academy of Sciences, Lanzhou 730000, China

ARTICLE INFO

Article history:
Received 25 March 2015
Received in revised form 5 February 2016
Accepted 5 March 2016
Available online 10 March 2016

Keywords:
Complementary relationship
Actual evapotranspiration
Pan evaporation
Asymmetry
Intensity of non-uniformity

ABSTRACT

The pan evaporation process is essential to understanding the climate change of pan evaporation. To study the physical process of pan evaporation and its interactions with the surrounding environment, an elaborate pan evaporation experiment was carried out by means of micrometeorological method in the arid region of northwest China, in which hourly pan evaporation was measured by E601B, Class A and D20 pans, the local actual evapotranspiration was measured using eddy correlation system. Our results show that the pan water surface and the surrounding land surface constitute a significant non-uniformity of heat and moisture, and the non-uniformity energy exchange between them has an important influence on pan evaporation rate. As the environmental humidity changes, daily actual evapotranspiration and pan evaporation rates have a contradictory tendency, with the relationship between these two evaporations presenting a clear asymmetrical complementary behavior. In addition, a simple pan non-uniformity intensity index (I_E) is defined as the ratio of pan evaporation to the Penman potential evaporation (LE_{ppman}) ($I_E = LE_{pan}/LE_{ppman}$). This index reflects the non-uniformity intensity between pan water and the surrounding land. Meanwhile, the comparison of complementary relationship corresponding to three types of pans shows that the degree of complementary relationship asymmetry linearly rises as the intensity of non-uniformity between pan and surrounding environment increases.

1. Introduction

The pan, as a routine evaporimeter at hydrological and meteorological stations, is the simplest, cheapest and most practical meteorological method to measure local atmospheric evaporation demand (Stanhill, 2002). Additionally, measurement of the pan evaporation is an important reference for water resource assessment, hydrological research, climatic zoning and monitoring evaporative climate change (Thom et al., 1981; Stanhill, 2002; Bruton et al., 2000; Sabziparvar et al., 2010). Studies on the pan evaporation in the past few decades showed that pan evaporation has had an obvious downward trend in many regions of the world (Peterson et al., 1995; Roderick and Farquar, 2002; Liu et al., 2004; Zuo et al., 2005; Rayner, 2007; Fu et al., 2009; Cong et al., 2009; McVicar et al., 2012, their Table 5). However, the explanations to this phenomenon vary. For example, some studies suggested that the reduction in solar irradiance that results from increasing cloud cover and/or aerosol quantity causes the decrease of pan evaporation (Peterson et al., 1995; Roderick and Farquar, 2002). Meanwhile, some studies considered that the decreased pan evaporation is attributed to the decreased near-surface wind speed (Rayner, 2007; Roderick et al., 2007; Limjirakan and Limsakul, 2012; Yang and Yang, 2012; McVicar et al., 2012). Although the above two explanations for the decline of pan evaporation are from different perspectives, they both imply the weakening land-air hydrological cycle (Peterson et al., 1995; Fu et al., 2009; Han et al., 2012). In contrast, some researchers believed that the declining trend of pan evaporation resulted from the reduction of vapor pressure deficit caused by the increase of air relative humidity in some regions (Brutsaert and Parlange, 1998; Lawrimore and Peterson, 2000; Ji and Zhou, 2011), although global observations of the near-surface air relative humidity are average, roughly constant (Dai,

* Corresponding author at: Bolong Chen and Hongchao Zuo, College of Atmospheric Sciences, Lanzhou University, 222 Tianshui South Road, Lanzhou 730000, China.
E-mail addresses: zuohch@lzu.edu.cn (H. Zuo), chenbl@lzu.edu.cn (B. Chen).

http://dx.doi.org/10.1016/j.agrformet.2016.03.002

2006; Willett et al., 2008). However, this conclusion implies the land-air hydrological cycle is accelerating (Shen et al., 2010), which has been supported by the fact that the actual soil evaporation is enhanced in some regions of the world after the increased precipitation in the same period (Dai et al., 1997; Karl and Knight, 1998; Liu et al., 2005; Brutsaert, 2006). There are two even contradictory conclusions on the climatic signals revealed by the declining trend in pan evaporation. Such situation drives researchers to explore the new answers from the physical process mechanism of pan evaporation and the relations among evaporation variables that are defined according to various observation and study approaches, such as actual evapotranspiration, reference evapotranspiration, pan evaporation and potential evaporation, and so on (Allen et al., 1998).

The complementary relationship initially proposed by Bouchet (1963) is considered as a key to solve this problem, and has been greatly developed and promoted over the past few decades (Morton, 1969, 1983; Brutsaert and Stricker, 1979; Brutsaert, 1982; Granger, 1989; Granger and Gray, 1990). The complementary relationship theory has also been widely tested and applied in different climatic zones and land surfaces (Brutsaert and Parlange, 1998; Szilagyi, 2001; Golubev et al., 2001; Haque, 2003; Ozdogan and Salvucci, 2004; Hobbins et al., 2004; Ramírez et al., 2005; Crago and Crowley, 2005; Yang et al., 2006; Huntington et al., 2011). However, most of these studies were based on the complementary relationship between empirical potential evaporation and actual evapotranspiration. Hence, some scholars pointed out that the complementary relationship is not reliable due to the lack of theoretical basis and the assumptions of strict evaporation conditions (Morton, 1983; Szilagyi, 2001). Some reports even said that the complementary relationship between potential evaporation and actual evapotranspiration is conditionally symmetrical (Kim and Entekhabi, 1998; McNaughton and Spriggs, 1989; Sugita et al., 2001).

Kahler and Brutsaert (2006) confirmed that the complementary relationship between daily actual evapotranspiration and Class A pan evaporation shows a significant asymmetry. Szilagyi (2007) pointed out that the degree of complementary relationship asymmetry between actual evapotranspiration and apparent potential evaporation is a function of surface temperature, not a constant. Meanwhile, Pettijohn and Salvucci (2006) found that the conductivity of canopy can affect the symmetry of complementary relationship. Furthermore, by building a two-dimensional physical model for Class A pan, they found that the atmospheric boundary depth and vegetation height can also affect the symmetry between pan evaporation and actual evaporation (Pettijohn and Salvucci, 2009). In addition, the evaporation area imposes significant impacts on the symmetry of complementary relationship (such as lakes, reservoirs, rivers, small ponds and pans). The open water body must have a certain size for the complementary relationship to become symmetric (Szilagyi and Jozsa, 2008).

Pans employed in measuring evaporation were not identical in different countries or regions across the world, such as Class A pan (in North American and Australia), GGI3000 (a sunken pan in Russia), BMO tank (in Britain), E601B pan and D20 pan (in China) (Fu et al., 2004; McVicar et al., 2012). Because the geometry size, installation method and structure of the pan have a significant influence on the measured results, the values measured by different types of pans were not equal on the same environmental background (Linacre, 1994; Fu et al., 2004; Martinez et al., 2006; Rotstayn et al., 2006; Yang and Yang, 2012). In the past decade, the evaporation process of Class A pan was studied in detail (Jacobs et al., 1998; Roderick et al., 2007, 2008a,b; Chu et al., 2010; Lim et al., 2012, 2013), however the careful study on other types of pans is rare. To understand the relationship between different types of pans evaporation and actual evapotranspiration, a field experiment was performed in the arid region of northwest China, where pan evaporation was simultaneously measured by D20, E601B and Class A pans. Actual evapotranspiration was observed with eddy correlation system. Simultaneously, micrometeorological method was adopted to observe the whole pans' evaporating process carefully. Our study has two objectives: (i) to analyze whether there is a complementary relationship between pan evaporation and actual evapotranspiration; (ii) to investigate the effect of different types of pans on the symmetry of complementary relationship.

2. Complementary relationship theory

The concept of complementary can be briefly summarized as follows: for a relatively large uniform surface (1–10 km) with minimal advection of heat and moisture, actual evapotranspiration (LE) and potential evaporation (LE_p) interact through land-atmosphere feedbacks, and are linked with each other by equilibrium evaporation, or wet environment evapotranspiration (LE_w). Here LE_w is the actual evapotranspiration in wet environment (with limited energy and adequate moisture). When moisture at the land surface is adequate, $LE = LE_p = LE_w$, and LE_w is only determined by the available energy which received by land surface. When the available energy maintains constant and the land surface gradually becomes dry, LE falls below LE_w and the sensible heat flux increases. This will gradually warm and dry the near-surface air, and saturation vapor pressure deficit will increase due to the lack of moisture, thus elevating LE_p. The complementary relationship between LE and LE_p can be expressed as:

$$b(LE_w - LE) = LE_p - LE_w \tag{1}$$

where b is a proportional coefficient to measure the impact of the change in actual evapotranspiration on potential evaporation. In other words, one-fold change in LE can cause b-fold changes in LE_p in opposite direction. When $b = 1$, Eq. (1) is symmetric complementary relationship, which implies that one unit decrease in LE results in one unit increase in LE_p; when $b \neq 1$, the relationship between LE and LE_p is asymmetric. Commonly, LE_w is estimated using the Priestley-Taylor equation (Priestley and Taylor, 1972; Brustaert and Stricker, 1979):

$$LE_w = \alpha \frac{\Delta}{\Delta + \gamma}(R_n - G_0) \tag{2}$$

where $\Delta (= de_0/dT)$ is the slope of the saturated vapor pressure curve corresponding to air temperature (kPa °C $^{-1}$), γ is psychrometric constant (kPa °C $^{-1}$), R_n is net radiation (W m^{-2}), G_0 is heat flux on the surface (W m^{-2}). α is the Priestley-Taylor coefficient. Commonly, α is used as a calibration coefficient; however, here α is fixed to the Priestley-Taylor original value of 1.26 to reduce the degrees of freedom (Brustaert and Stricker, 1979; Huntington et al., 2011). Potential evaporation as an index is commonly used to estimate the air evaporative demand. However, it only represents the evaporation under some special assumed conditions and is difficult to be measured directly, so some empirical formulas are generally employed to determine local potential evaporation (Donohue et al., 2010; McMahon et al., 2013).

The complementary relationship between pan evaporation and actual evapotranspiration is researched by replacing LE_p with pan evaporation, and can be expressed as:

$$b(LE_w - LE) = LE_{pan} - LE_w \tag{3}$$

Here b is proportional coefficient; $b \neq 1$ means complementary relationship is asymmetrical. The relationship between some physical variables can become more straightforward in normalized form. In order to clarify the relationship, the Formula (3) is normalized following the methods from Kahler and Brutsaert (2006) and Huntington et al. (2011) who scaled LE and LE_{pan} with LE_w

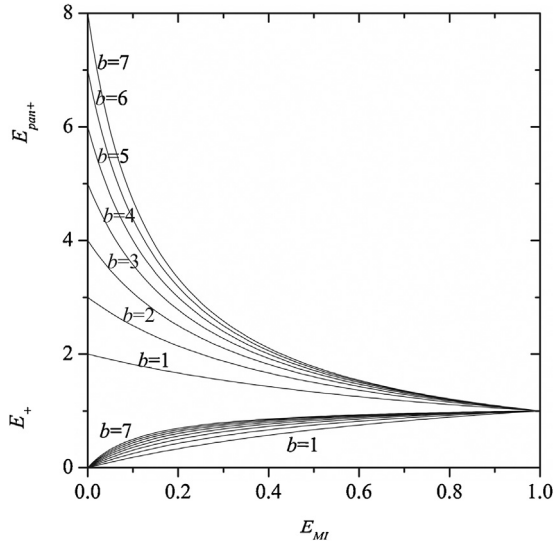

Fig. 1. Complementary relationship between dimensionless variables E_+ and E_{pan+} with different b, where $E_+ = LE/LE_w$, $E_{pan+} = LE_{pan}/LE_w$; as x moves from left to right, the environment gets wet and the humidity index E_{MI} increases accordingly.

and got two dimensionless variables, namely $E_+ = LE/LE_w$ and $E_{pan+} = LE_{pan}/LE_w$.

Generally, both air relative humidity and soil volumetric water content can be used to measure the humidity of local environment, but it is difficult to directly reflect the complicated evaporation process with this single physical variable (Kahler and Brutsaert, 2006; Huntington et al., 2011). Under normal circumstances, a strong actual evapotranspiration can make the air moist, and also can inhibit pan evaporation rate at the same time. To reflect both the changes in actual evapotranspiration and pan evaporation simultaneously, an environmental moisture index (E_{MI}) is defined as the ratio of LE to LE_{pan}:

$$E_{MI} = LE/LE_{pan} \tag{4}$$

E_{MI} can describe the degree of the approximation of evaporation surface to potential evaporation conditions. As pan can receive radiation through walls and bottom and is free from water restrictions, its evaporation is greater than the actual evaporation, usually $0 \le LE < LE_{pan}$, and $0 \le E_{MI} < 1$. When E_{MI} tends to 0, it means the environment is drying; when E_{MI} tends to 1, it means the environment is wetting. Different types of pan demonstrate different evaporation rates in the same environment, and thus, E_{MI} depends on pan type. Noting E_{MI} is a factor linking pan evaporation and the environment and it does not affect the respective relationship between actual evapotranspiration and corresponding pan evaporation.

E_{MI} is used to create the function for the dimensionless variables E_+ and E_{pan+}, and Formula (3) will be translated into the following two functions:

$$E_+ = \frac{(1+b)E_{MI}}{1+bE_{MI}} \tag{5}$$

and

$$E_{pan+} = \frac{1+b}{(1+bE_{MI})} \tag{6}$$

The changes in E_+ and E_{pan+} along with E_{MI} are plotted in the same graph (Fig. 1). It can be drawn that when $b = 1$, the curves of E_+ and E_{pan+} constitute a symmetric complementary relationship; when $b \neq 1$, the curves constitute an asymmetric complementary relationship (Only results of $b > 1$ are plotted in Fig. 1).

The proportional coefficient b is determined with the least square method using the observational data. Kahler and Brusteart (2006) investigated the Class A pan data collected from two different sites, and found b was 4.33 for *Konza Prairie* and 6.88 for *Washita basin*. Thus, they recommended that 5 might be a relatively appropriate value for b. Pettijohn and Salvucci (2009) utilized Class A pan model and showed that b ranged from 3.3 to 6.2. Huntington et al. (2011) also pointed out that b might vary from 4 to 10 when analyzing Class A pan data. Their studies showed that the value of b might be affected by the studied area and spatial characteristics (such as arid and humid areas). In addition, the radiation received by the pan wall and advection energy can influence the energy of water in the pan, and the different types of pan may also impose different impacts, contributing to different values of b. These researches and ours are summarized in Table 1, in terms of observational site, underlying surface, pan type, research approach and key results.

3. Experiment set-up and data

3.1. Field introduction

The experimental site (Longitude, 103°55′E; Latitude, 37°45′N; Elevation, 1563 m) is located at the southern border of Tengger Desert which is the fourth largest desert in China, belonging to Alxa Left League, Inner Mongolia Autonomous Region. This area has a typical northern temperate arid climate. Averaged from 1971 to 2000, it has a mean annual precipitation of 35.2 mm mainly in May–September, mean annual relative humidity of 33%, mean annual wind speed of 3.2 m/s at 10 m height, and mean annual D20 pan evaporation of 3400 mm. Its mean monthly air temperatures range from −10.5 °C in December to 27.6 °C in July. The underlying surface is scattered sparse perennial Alhagisparsifolia and sparse low weeds. The albedo of underlying surface is 0.28 during dry period of Alhagisparsifolia, 0.23 during growth period of Alhagisparsifolia, and minimum 0.15 when the soil is saturated by rainfall.

There were 4 substantial rainfalls during the experiment, and 20.0 mm on June 27, 36.0 mm on days of July 29 and 30, 12.3 mm on September 1 and 8.5 mm on September 11. These were extensive precipitation for the arid area, and changed the humidity of local environment evidently. The soil dried up from saturated condition in 3–4 days after rainfall, for the great potential evaporation in the arid area. The occasional large precipitation in spatial scale and amount provides favorable conditions for study on complementary relationship in the arid environment.

3.2. Pan experiment design and measurement

The pan evaporation is measured by three types of pans located at the center of the field (see Fig. 2a), including Class A, E601B and D20 pans. The details of the sensors, installation and observation programs are as follows: two standard Class A pans (noted as Class A_01 and Class A_02) as shown in Fig. 1b, 121 cm in diameter, 25 cm deep, and located on a wooden platform about 15 cm above the ground. The water depth in both pans is about 20 cm. Class A_01 pan was used to measure the water temperature at the depth of 5, 10 and 20 cm, with three platinum wire sensors (107; Campbell) which were fixed on a steel support set in pan center. Class A_02 pan was used to observe pan evaporation rate by evaporation gauge (Novalynx 255–100) which could monitor water level changing. This evaporation gauge, which consists of float, pulley, and counter weight attached to a precision potentiometer mounted through a gear assembly in weather proof housing, was installed in the pan water. The pan evaporation rate sampling frequency is every 10 min.

Three standard E601B pans (noted as E601B_01, E601B_02 and E601B_03) were installed according to the Standards for

Table 1
Summary of relevant studies about complementary relationship between actual evapotranspiration and pan evaporation (the current paper is added for completeness). EBBR: energy budget with Bowen ratio method; EC: eddy correlation system; Epan: pan evaporation; Tw: temperature of water in the pan; (1): asymmetrical complementary; (2): asymmetrical complementary and its relationship with the pan non-uniformity.

Study	Location	Landscape	Pan type and observation variables	Evapotranspiration	b	Key results
1 Kahler and Brutsaert (2006)	Konza Prairie, Kansas, U.S.	Grassland	Class A, Epan	EBBR	4.33	(1)
	Washita basin, Oklahoma, U.S.	Rangeland	Class A, Epan	EBBR	6.88	(1)
2 Pettijohn and Salvucci (2009)			Class A, simulated Epan	simulated	3.3-6.2	(1)
3 Huntington et al. (2011)	Great Salt Lake, Nevada, U.S.	Shrubland	Class A, Epan	EC	4.0-10.0	(1)
4 Ma et al. (2015)	Naqu and Amdo, Tibetan Plateau, China	Alpine steppe	E601 and D20, Epan	EBBR	2.359, 3.863	(1)
5 This study	Alxa, Inner Mongolia, China	Alhagisparsifolia and Sparse low weeds	Class A, E601B and D20, Epan, Tw	EC	2.22, 3.43 and 4.40	(1) and (2)

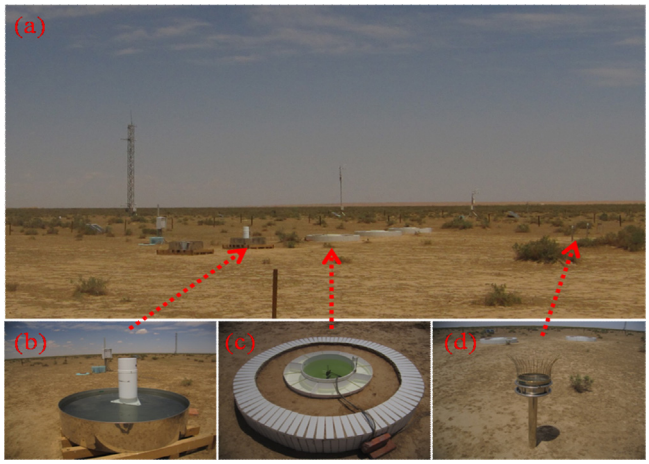

Fig. 2. Observation site and instruments. (a) site overview, micrometeorological tower, Eddy Correlation System and 4-Component Net Radiation Sensor, (b) Class A pan, (c) E601B pan, (d) D20 pan.

Meteorological Instruments Observation of China Meteorological Administration (CMA). The E601B pan was made of fiberglass, with diameter 0.6 m and depth 0.6 m, and was sunk into the ground (see Fig. 2c). E601B_01 was used to measure the water temperature at the depth of 5, 10, 20 and 40 cm with the similar steel support used in Class A _01. E601B_02 pan was used to observe pan evaporation rate. Evaporation rate in the E601B pan was calculated based on the height difference of water surface at two adjacent hours via a rim micrometer (resolution 0.1 mm) fixed on the brim of pan. The E601B_03 was for water storage and used to replenish the water in other pans (to ensure that replenish water was at a similar temperature to the water in the pans).

Two D20 pans (noted as D20_01 and D20_02) made of galvanized copper and widely used throughout China were used. They are 0.2 m in diameter and 0.1 m deep, containing water to a depth of about 0.04 m, and are located on a steel platform about 0.7 m above the ground (see Fig. 2d). D20_01 pan was used to measure pan evaporation and D20_02 pan was used to observe water temperature by a mercury thermometer (resolution 0.2 °C) fixed in center of water at the depth of 0.02 m.

Water surface temperatures of all pans were measured hourly by hand-hold infrared thermometer (resolution 0.2 °C). Throughout the experiment, every non-automatic measurement was performed hourly and automatic measurement was done successively. All observations were 24-h measurements both day and night, except on some adverse weather (e.g., rain and sand storm) days when non-automatic observation maybe absent. All pans were supplemented at 21:00 every day as follows. At first, Class A_02 was supplemented with the water in Class A_01. Then Class A_01, E601B_01, E601B_02, D20_01 and D20_02 were supplemented with water from E601B_03 which was replenished with underground water. This ensured that the temperature of the replenished water was as close as possible to that of pan water, because the temperature of the water can have an impact on the rate of pan evaporation (Jacobs et al., 1998; Martinez et al., 2006; McVicar et al., 2007).

3.3. Meteorological equipment

One 12 m high meteorological tower (see Fig. 2e) was set up in the observing experiment field. There are 4-level air temperature and relative humidity sensors at heights of 0.5, 1.5, 2, 10 m (HMP45C; Vaisala), 3-level wind speed sensors at heights of 0.5, 2, 10 m (010C; Metone) and a wind direction sensor at 10 m (W200P; Vector) on the tower. Moreover, a 4-compentent net radiation sensor (CNR1; Kipp&Zonen) is installed at 1.5 m height for radiation observation, which is 20 m away from the tower in the south. Two sets of 3D supersonic anemometer (CSAT3; Campbell) and open-way gas analyzers for CO_2 and H_2O (LI7500; Campbell) are installed for turbulence observation at heights of 3 m and 6 m near the tower. The gauge (52202 of RM. Young) is used for precipitation measurement. The devices for soil temperature (109; Campbell) and water content (CS616; Campbell) are set in the soil at depths of 0.05, 0.1, 0.2, 0.4 and 0.8 m, and soil heat flux plates (HFP01SC2L; Campbell) are installed at depths of 0.05, 0.1, and 0.2 m, all these sensors are set about 10 m from the tower in the south.

3.4. Data processing

The observed energy closure ratio in the surface layer is 73.9% during the experiment. The Bowen ratio method is used to correct the sensible heat and latent heat fluxes for conservation of energy (Twine et al., 2000; Forken, 2008; Gallego-Elvira et al., 2010). The Bowen ratio is determined by the measured fluxes with eddy correlation system, ensuring the Bowen-ratio consistency before and after processing the measurements. Daily average meteorological measurements of air temperature, air relative humidity, air pressure, wind speed, ground heat flux, upward and downward long wave and upward and downward short wave radiations are used to calculate potential evaporation (LE_{pman}) by Penman formula with Rome wind function as $0.26(1 + 0.56U_2)$, where U_2 is the wind speed at 2 m height (Brutsaert, 1982), and the equilibrium evapotranspiration (LE_w) is calculated by Priestley-Taylor equation (Priestley and Taylor, 1972).

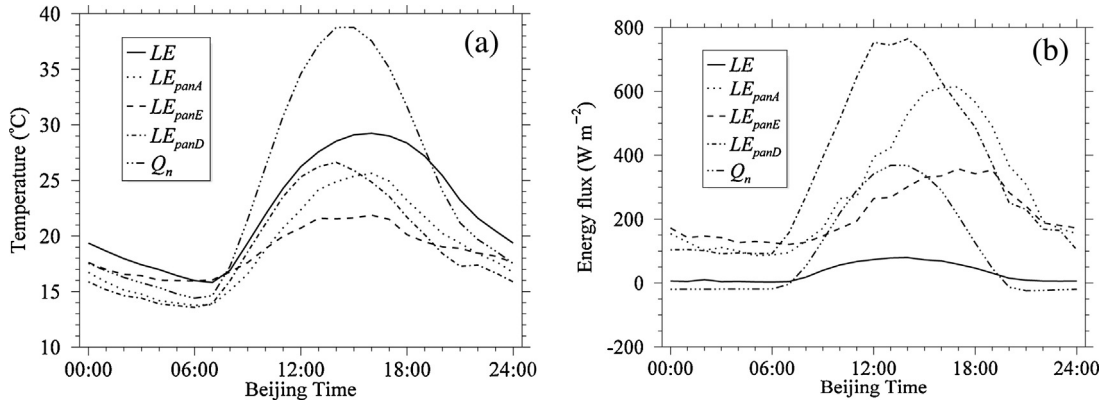

Fig. 3. Average temperature, evaporation and energy flux during 57 days (a) average hourly temperatures of land surface (T_s), pans water surface (T_A, T_E and T_D for Class A, E601B and D20 pan, respectively) and air at a height of 0.5 m (T_a); (b) average hourly evaporation of pans water (LE_{panA}, LE_{panE} and LE_{panD}), available energy ($Q_n = R_n - G_0$) and actual evaporation (LE) of land surfaces.

The data was collected from 10 June to 28 September 2012, a total of 110 days. Only 57 days are selected from all 110 days, as all days on which the observation was interrupted by adverse weather (e.g., rain and sand storm) or on which not all relevant observations were synchronous are excluded.

4. Results

4.1. Major observational differences among evaporation pans

Evaporation pan is artificial water surface that is small enough in size not to be able to influence its background conditions. However, the water in the pan and the surrounding environment constitute a significant non-uniformity due to the differences in the surface temperature, moisture, albedo and so on. The non-uniformity between pan water and surrounding land surface is the most strong in the arid area. The average temperatures of land surface, water surface and air at 0.5 m height for 57 days are compared (Fig. 3a). Water surface temperatures of three types of pans are all lower than the temperature of land surface in daytime, and water surface temperatures of Class A and D20 pans are lower than the temperature of land surface in nighttime, but water surface temperature of E601B pan is higher than the temperature of land surface in nighttime. Water surface temperatures of three types of pans are all lower than the air temperature observed at 0.5 m above the ground in whole daytime. The maximum water temperatures of D20, Class A, and E601B pans are approximately happened at 14:00, 16:00, and 16:00, respectively. D20 pan has the highest maximum water temperature, while E601B pan the lowest.

Fig. 3b demonstrates the averaged land actual evapotranspiration and three types of pans evaporation fluxes. It shows that the pan evaporations are greater than actual evapotranspiration, which is restricted by soil available water. The pan evaporations are also greater than the observed land available energy ($Q_n = R_n - G_0$, where R_n and G_0 are net radiation and land surface soil heat flux, respectively) at the daily scale. The pan evaporation of D20 pan is the largest, with its maximum is about 770 W m^{-2} at 14 o'clock, whose diurnal trend is similar to that of available energy. It is because the D20 pan has the smallest water body (McVicar et al., 2007). For this reason, the energy exchange in D20 pan is the strongest and its response is the quickest. Although the geometrical structure of Class A pan is similar to D20 pan, its water body is much larger than that in D20 pan. So its evaporation maximum is about 610 W m^{-2} at 17 o'clock and its diurnal trend has a delay about 2 h for D20 pan. Finally, the evaporation maximum of E601B is the least, about 360 W m^{-2}, its evaporation maximum appears at 17 o'clock, and its diurnal variation pattern is different, due to its deepest water body and different installation method (i.e., sunk into the ground) from the other two types of pans.

4.2. Complementary relationship between LE_{pan} and LE

The relationships between daily evaporation of three types of pans and actual evaporation are shown in Fig. 4. For E601B (Fig. 4a, b), the relationship between daily E601B pan evaporation LE_{panE} and actual evapotranspiration LE observed by eddy correlation system against moisture index $E_{MI} = LE/LE_{panE}$ is shown in Fig. 4a. From left to right in the figure, actual evapotranspiration LE increases, while pan evaporation LE_{panE} decreases along with the increasing humidity index E_{MI}; and vice versa. Referring to the weather evolution during the observation, after heavy precipitation, soil gradually dries, land surface moisture falls, and environment humidity index E_{MI} becomes lower. Corresponding to this process, the actual evapotranspiration decreases from 100 W m^{-2} to almost zero, and the E601B pan evaporation gradually increases to a maximum of 350 W m^{-2} from the initial 100 W m^{-2}. It shows that LE_{panE} and LE complements each other overall. However, although such a relationship is very clear, the points are quite dispersed, especially the points of pan evaporation rate. After LE_{panE} and LE are normalized by wet environment evaporation LE_w, the relationship between LE_{panE}/LE_w and LE/LE_w against moisture index E_{MI} is presented in Fig. 4b. It is found that there is a very prominent complementary relationship between LE_{panE}/LE_w and LE/LE_w. This finding is similar to previous conclusions (Kahler and Brusteart, 2006; Huntington et al., 2011). Two groups of points in Fig. 4b are fitted using Formulas (5) and (6) as a whole with the least squares method, and the optimal b is 2.22. The relationship between actual evapotranspiration and E601B pan evaporation is asymmetric. As the environment humidity changes, corresponding to every unit volume change in actual evapotranspiration, pan evaporation changes by 2.22 times, but with an opposing trend. For Class A pan (Fig. 4c, d) and for D20 pan (Fig. 4e, f), they all show the asymmetric complementary relationship as E601B pan (Fig. 4a, b), and the optimal b is 3.43 and 4.40 respectively.

In terms of the complementary relationship of these three types of pans, despite the same variation in actual evapotranspiration, the three pans have substantial different variations in evaporation. With the environment drying, the evaporation of E601B pan increases from 100 to 350 W m^{-2}, Class A pan from 120 to 500 W m^{-2}, and D20 pan from 150 to 600 W m^{-2}.

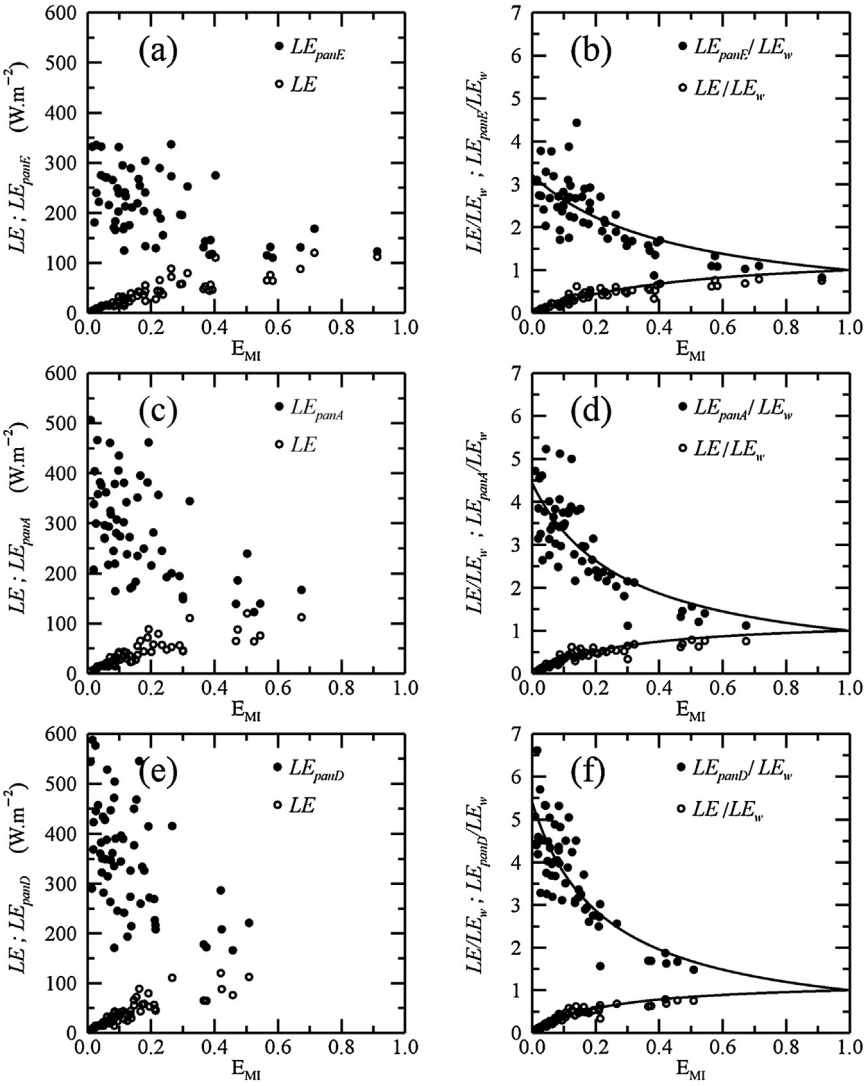

Fig. 4. Daily actual evaporation LE (W m^{-2}) and the evaporation LE_{panE} (W m^{-2}) plotted against moisture index E_{MI}. (a), (b), respectively, are the measured and normalized results for E601B pan with b = 2.22; (c), (d) for Class A pan with b = 3.43; and (e), (f) for D20 pan with b = 4.40.

As indicated by Fig. 4b, d, f, the points corresponding to three normalized pans evaporation LE_{pan}/LE_w compress leftward and extend upward successively. The reason for leftward movement lies in that humidity index E_{MI} is a relative parameter determined by the respective pan evaporation, and in the case of the same LE, a greater LE_{pan} leads to a smaller E_{MI}. Since $LE_{panD} > LE_{panA} > LE_{panE}$, the E_{MI} of D20 pan is the smallest, followed by Class A pan and then E601B pan under the same conditions.

Moreover, compared with the consistency between actual evapotranspiration and function (6), the consistency between pan evaporation and function (6) is slightly weaker. Some points are scattered around the curve, especially in the case of strong pan evaporation at low environment humidity index. This also implies that the factors affecting pan evaporation may be different from those affecting land surface evapotranspiration.

4.3. Pan non-uniformity with its environment and asymmetry of complementary

In order to quantitatively measure the degree of the non-uniformity between pan water and surrounding land surface by employing Penman potential evaporation as the standard, a pan non-uniformity intensity index, I_E, is defined as:

$$I_E = LE_{pan}/LE_{ppman} \tag{7}$$

To reduce the degrees of freedom, here I_E is assumed as constant during our experiment.

For E601B, Class A, and D20, the pan evaporation increases gradually (such as $LE_{panD} > LE_{panA} > LE_{panE}$). When the non-uniformity intensity between pan and the surrounding environment is enhanced, the LE_{pan} increases, and the corresponding non-uniformity intensity index I_E also rises. According to the Formula (7), the I_E corresponding to E601B, Class A and D20 pan is 1.26, 1.72 and 2.08 respectively using linear analysis between observed pan evaporation and calculated LE_{ppman}.

Fig. 5 is the relationship between proportional coefficient b and pan non-uniformity intensity index I_E, which shows that b is direct ratio with I_E. This reveals that the asymmetry of complementary relationship between pan evaporation and actual evapotranspiration is linearly related to the non-uniformity intensity.

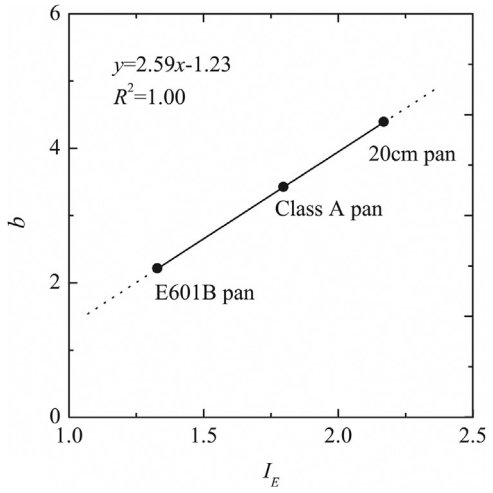

Fig. 5. Proportional coefficient b in complementary relationship against the pan non-uniformity intensity index (I_E). The solid line is linearly fitted, and the dotted line is the expansion line from the solid line.

5. Discussion

Our results suggest that the three types of pan evaporation respectively present a clear asymmetrical complementary relationship with actual evapotranspiration (Fig. 4). However, they have obvious difference, such as different proportional coefficient b for different evaporation pan. Existing studies have also shown that the proportional coefficients vary with the different underlying surfaces and the climatic zones (Kahler and Brusteart, 2006; Pettijohn and Salvucci, 2009; Huntington et al., 2011; Ma et al., 2015). This is determined by the characteristics of interaction between the pan and the surrounding environment. Pan evaporation process is determined by the non-uniformity between pan water and surrounding land surface, which is proved by our observation that the observed temperatures and evaporations of three pans water are evidently different in three aspects of amplitude, phase and pattern. The non-uniformity will lead to the horizontal energy exchange between the water body in evaporation pan and surrounding environment (Jacobs et al., 1998; Zuo et al., 2005, 2006; Martinez et al., 2006; Chen et al., 2013; Lim et al., 2012, 2013). First, the pan gains sensible heat energy from the air above it; the sensible heat energy comes from the surrounding land surface by turbulence and is then advected to the air above the pan. Furthermore, the pan water body exchanges energy with surrounding land surface by other ways, such as long wave radiation and heat conductivity. The way and degree of energy exchange between the pan and surrounding environment are closely related to the geometrical structure and principle of evaporation pan, and much, even greatly, different from one another. Affected by this energy exchange, the stronger the non-uniformity is and the less the water amount inside the evaporation pan is, the larger the pan evaporation is and the faster the pan responds to surrounding environment.

The implication is that the proportional coefficient b has a good linear relationship with the non-uniformity intensity between pans and surrounding environment. Assuming that the linear relationship between them remains constant, we can make further discussion on the extension of both sides. As shown by the dotted line in Fig. 5, when the non-uniformity intensity index I_E increases, and the corresponding proportional coefficient b increases as well, so does the evaporation rate. This means that the pan evaporation will grow evidently when the non-uniformity intensity between pan water and the surrounding land gradually increases. For example, in the extreme situation like a drop of water in arid environment, it evaporates out very quickly. There are water bodies of various sizes in natural environment that could be regarded as evaporation pans in different sizes. As discussed above, pan non-uniformity intensity index depends on its structure and principle, mainly its amount and the exposed area of pan water. The water body is reduced continuously meaning its non-uniformity intensity rises. That is why small and shallow water body has a greater amount of evaporation at the same environment. On the contrary, as the size of water body keeps increasing, I_E will decrease, so will the evaporation. When water body expand bigger enough, I_E will fall to 1, then the water surface evaporation and the potential evaporation will be equal (such as lake, or large-scale water surface), and the non-uniformity between water and environment will get minimal. In this case, based on the linear function obtained with regression method, the value of proportional coefficient b is 1.36. However, it is not consistent with the result of $b = 1$ from Bouchet's (1963) hypothesis.

Finally, the physical model of pan evaporation is sketched out from the research to date. The non-uniformity is formed between pan water and surrounding land surface when the atmospheric evaporation demand is measured with evaporation pan, and then the pan evaporation process is determined by the non-uniformity, and furthermore the non-uniformity varies according to pan structure, underlying surface, climatic region, and so on. Attention must be paid to the effect of the non-uniformity when the researches and applications about pan evaporation are made. Focus should be concentrated on the researches below: (i) how to measure quantitatively the non-uniformity, and its relation with pan structure, underlying surface, climatic region, and so on; (ii) how to eliminate the effect of the non-uniformity during researches and applications on pan evaporation.

Of course, this study is based on the experiment in arid regions of northwest China, and the results are calibrated only in this area, including non-uniformity intensity between pan and surrounding environment and the complementary relationship asymmetry determined by the non-uniformity. Then, whether these results are suitable for other climate zones (such as semi-humid areas, wet areas, and so on) still needs further observation and verification.

6. Conclusion

In this work, a pan evaporation experiment was carried out in the arid area of northwest China, which was comprised of E601B, Class A and D20 pans. Furthermore, the interactions between pan and the surrounding environment were measured by means of micrometeorological method. The relationship between pan evaporation and actual evapotranspiration was analyzed at daily scale, and the impact of different types of pans on the relationship was also investigated.

From E601B pan to Class A pan to D20 pan, the non-uniformity between the pan and the surrounding environment is different. The observed temperatures and evaporations of three pans water are evidently different in both amplitude and trend. All evaporation process measurements during the experiment show that, with the increase of humidity index E_{MI}, the average daily pan evaporation decreases, while the daily actual evapotranspiration increases. Therefore, the three types of pan evaporation respectively present a clear asymmetrical complementary relationship with actual evapotranspiration.

A pan non-uniformity intensity index I_E is defined by the ratio of pan evaporation to Penman potential evaporation ($I_E = LE_{pan}/LE_{ppman}$) to quantitatively measure the non-uniformity between pans and surrounding environment. From E601B pan to Class A pan, and to D20 pan, the asymmetry of the asymmetrical complementary relationship between pan evaporation and actual

evapotranspiration increases gradually. Furthermore, a good linear relationship is found between non-uniformity intensity and the proportional coefficient *b* of the corresponding asymmetrical complementary relationship.

Acknowledgements

This study was supported by the Special Meteorological Foundation of China (Grant GYHY201106043), the National Basic Research Program of China '973' Program (Grant 2012CB956200), the National Natural Science Foundation of China (Grant 41075006 and 41275019) and the Opening Fund of Key Laboratory of Land Surface Process and Climate Change in Cold and Arid Regions-Chinese Academy of Sciences (LPCC201402). The authors are grateful to the Agricultural and Forest Meteorology editors and two anonymous reviewers whose comments contributed to important improvements.

References

Allen, R.G., Pereira, L.S., Raes, D., Smith, M., 1998. Crop Evapotranspiration Guide Lines for Computing Crop Water Requirements. FAO Irrigation and Drainage, Rome, Italy (Paper 56).
Bouchet, R.J., 1963. Évapotranspiration réelleet potentielle significationc limatique. Int. Assoc. Sci. Hydrol. 62, 134–142.
Bruton, J.M., McClendon, R.W., Hoogenboom, G., 2000. Estimating daily pan evaporation with artificial neural networks. Trans. Am. Soc. Agric. Eng. 43 (2), 491–496.
Brutsaert, W., Parlange, M.B., 1998. Hydrologic cycle explains the evaporation paradox. Nature 396, 30.
Brutsaert, W., Stricker, H., 1979. An advection-aridity approach to estimate actual regional evapotranspiration. Water Resour. Res. 15, 443–450.
Brutsaert, W., 1982. Evaporation into the Atmosphere: Theory, History and Applications. Springer, New York, pp. 299.
Brutsaert, W., 2006. Indications of increasing land surface evaporation during the second half of the 20th century. Geophys. Res. Lett., 33, http://dx.doi.org/10.1029/2006GL027532 (L20403).
Chen, B.L., Zuo, H.C., Gao, X.Q., Yang, X.G., Ren, P.C., Chen, J.W., 2013. A mathematical and physical model study on the 20 cm pan evaporation (in Chinese). Chin. J. Geophys. 56, 422–430.
Chu, C.R., Li, M.H., Chen, Y.Y., Kuo, Y.H., 2010. A wind tunnel experiment on the evaporation rate of Class A evaporation pan. J. Hydrol. 381, 221–224.
Cong, Z.T., Yang, D.W., Ni, G.H., 2009. Does evaporation paradox exist in China? Hydrol. Earth Syst. Sci. 13 (3), 357–366.
Crago, R., Crowley, R., 2005. Complementary relationships for near-instantaneous evaporation. J. Hydrol. 300, 199–211.
Dai, A.G., Fung, I.Y., Genio, A.D.D., 1997. Surface observed global land precipitation variations during 1900–88. J. Clim. 10, 2943–2962.
Dai, A.G., 2006. Recent climatology, variability, and trends in global surface humidity. J. Clim. 19 (15), 3589–3606.
Donohue, R.J., McVicar, T.R., Roderick, M.L., 2010. Assessing the ability of potential evaporation formulations to capture the dynamics in evaporative demand within a changing climate. J. Hydrol. 386 (1–4), 186–197, http://dx.doi.org/10.1016/j.jhydrol.2010.03.020.
Forken, T., 2008. The energy balance closure problem: an overview. Ecol. Appl. 18, 1351–1367.
Fu, G.B., Liu, C., Chen, S., Hong, J., 2004. Investigating the conversion coefficients for free water surface evaporation of different evaporation pans. Hydrol. Processes 18, 2247–2262.
Fu, G.B., Charles, S.P., Yu, J.J., 2009. A critical overview of pan evaporation trends over the last 50 years. Clim. Change 97, 193–214.
Gallego-Elvira, B., Baille, A., Martin-Gorriz, B., Martinez-Alvarez, V., 2010. Energy balance and evaporation loss of an agricultural reservoir in a semi-arid climate (south-eastern Spain). Hydrol. Processes 24, 758–766.
Golubev, V.S., Lawrimore, J.H., Groisman, P.Y., Speranskaya, N.A., Zhuravin, S.A., Menne, M.J., Peterson, T.C., Malone, R.W., 2001. Evaporation changes over the contiguous United States and the former USSR: a reassessment. Geophys. Res. Lett. 28, 2665–2668.
Granger, R.J., Gray, D.M., 1990. Examination of Morton's CRAE model for estimating daily evaporation from field-sized areas. J. Hydrol. 120, 309–325.
Granger, R.J., 1989. A complementary relationship approach for evaporation from nonsaturated surfaces. J. Hydrol. 111, 31–38.
Han, S.J., Xu, D., Wang, S.L., 2012. Decreasing potential evaporation rends in China from 1956 to 2005: accelerated in regions with significant agricultural influence? Agric. Forest Meteorol. 154–155, 44–56.
Haque, A., 2003. Estimating actual areal evapotranspiration from potential evapotranspiration using physical models based on complementary relationships and meteorological data. Bull. Eng. Geol. Env. 62, 57–63.
Hobbins, M.T., Ramírez, J.A., Brown, T.C., 2004. Trends in pan evaporation and actual evapotranspiration across the conterminous U.S.: paradoxical or complementary? Geophys. Res. Lett. 31, L13503, http://dx.doi.org/10.1029/2004GL019846.
Huntington, J.L., Szilagyi, J., Tyler, S.W., Pohll, G.M., 2011. Evaluating the complementary relationship for estimating evapotranspiration from arid shrublands. Water Resour. Res. 47, W05533, http://dx.doi.org/10.1029/2010WR009874.
Jacobs, A.F.G., Heusinkveld, B.G., Lucassen, D.C., 1998. Temperature variation in a class A evaporation pan. J. Hydrol. 206, 75–83, http://dx.doi.org/10.1016/S0022-1694(98)00087-0.
Ji, Y.H., Zhou, G.S., 2011. Important factors governing the incompatible trends of annual pan evaporation: evidence from a small scale region. Clim. Change 106, 303–314.
Kahler, D.M., Brutsaert, W., 2006. Complementary relationship between daily evaporation in the environment and pan evaporation. Water Resour. Res. 42, W05413, http://dx.doi.org/10.1029/2005WR004541.
Karl, T.R., Knight, R.W., 1998. Secular trends of precipitation amount, frequency, and intensity in the USA. Bull. Am. Meteorol. Soc. 79, 231–241.
Kim, C.P., Entekhabi, D., 1998. Feedbacks in the land-surface and mixed-layer energy budgets. Boundary Layer Meteorol. 88, 1–21.
Lawrimore, Jay H., Peterson, Thomas C., 2000. Pan evaporation trends in dry and humid regions of the United States. J. Hydrometeor. 1, 543–546.
Lim, W.H., Roderick, M.L., Hobbins, M.T., Wong, S.C., Groeneveld, P.J., Sun, F.B., Farquhar, G.D., 2012. The aerodynamics of pan evaporation. Agric. Forest Meteorol. 152, 31–43, http://dx.doi.org/10.1016/j.agrformet.2011.08.006.
Lim, W.H., Roderick, M.L., Hobbins, M.T., Wong, S.C., Farquhar, G.D., 2013. The energy balance of a US Class A evaporation pan. Agric. Forest Meteorol. 182-183, 314–331, http://dx.doi.org/10.1016/j.agrformet.2013.07.001.
Limjirakan, S., Limsakul, A., 2012. Trends in Thailand pan evaporation from 1970 to 2007. Atmos. Res. 108, 122–127.
Linacre, E.T., 1994. Estimating U. S. Class A pan evaporation from few climate data. Water Int. 19, 5–14, http://dx.doi.org/10.1080/02508069408686189.
Liu, B.H., Xu, M., Henderson, M., Gong, W.G., 2004. A spatial analysis of pan evaporation trends in China, 1955–2000. J. Geophys. Res. 109, D15102, http://dx.doi.org/10.1029/2004JD004511.
Liu, B.H., Xu, M., Henderson, M., Qi, Y., 2005. Observed trends of precipitation amount, frequency, and intensity in China, 1960–2000. J. Geophys. Res. 110, D08103, http://dx.doi.org/10.1029/2004JD004864.
Ma, N., Zhang, Y., Szilagyi, J., Guo, Y., Zhai, J., Gao, H., 2015. Evaluating the complementary relationship of evapotranspiration in the alpine steppe of the Tibetan Plateau. Water Resour. Res. 51, http://dx.doi.org/10.1002/2014WR015493.
Martinez, J.M.M., Alvarez, V.M., Gonzalez-Real, M.M., Baille, A., 2006. A simulation model for predicting hourly pan evaporation from meteorological data. J. Hydrol. 318, 250–261, http://dx.doi.org/10.1016/j.jhydrol.2005.06.016.
McMahon, T.A., Peel, M.C., Lowe, L., Srikanthan, R., McVicar, T.R., 2013. Estimating actual, potential, reference crop and pan evaporation using standard meteorological data: a pragmatic synthesis. Hydrol. Earth Syst. Sci. 17, 1331–1363, http://dx.doi.org/10.5194/hess-17-1331-2013.
McNaughton, K.G., Spriggs, T.W., 1989. An evaluation of the Priestley-Taylor equation and the complementary relation using results from a mixed-layer model of the convective boundary layer. Estimation of Areal Evapotranspiration, 177. IAHS, Vancouver, B.C., Canada, pp. 89–104.
McVicar, T.R., Van Niel, T.G., Li, L.T., Hutchinson, M.F., Mu, X.M., Liu, Z.H., 2007. Spatially distributing monthly reference evapotranspiration and pan evaporation considering topographic influences. J. Hydrol. 338 (3–4), 196–220, http://dx.doi.org/10.1016/j.jhydrol.2007.02.018.
McVicar, T.R., Roderick, M.L., Donohue, R.J., Li, L.T., Van Niel, T.G., Thomas, A., Grieser, J., Jhajharia, D., Himri, Y., Mahowald, N.M., Mescherskaya, A.V., Kruger, A.C., Rehman, S., Dinpashoh, Y., 2012. Global review and synthesis of trends in observed terrestrial near-surface wind speeds: implications for evaporation. J. Hydrol. 416–417, 182–205.
Morton, F.I., 1969. Potential evaporation as a manifestation of regional evaporation. Water Resour. Res. 5, 1244–1255.
Morton, F.I., 1983. Operational estimates of areal evapotranspiration and their significance to the science and practice of hydrology. J. Hydrol. 66, 1–76.
Ozdogan, M., Salvucci, G.D., 2004. Irrigation-induced changes in potential evapotranspiration in southeastern Turkey: test and application of Bouchet's complementary hypothesis. Water Resour. Res. 40, W04301, http://dx.doi.org/10.1029/2003WR002822.
Peterson, T.C., Golubev, V.S., Groisman, P.Y., 1995. Evaporation losing its strength. Nature 377, 687–688.
Pettijohn, J. Cory, Salvucci, Gudio D., 2006. Impact of an unstressed canopy conductance on the Bouchet-Morton complementary relationship. Water Resour. Res. 42, W09418, http://dx.doi.org/10.1029/2005WR004385.
Pettijohn, J. Cory, Salvucci, Guido D., 2009. A new two-dimensional physical basis for the complementary relation between terrestrial and pan evaporation. J. Hydrometeor. 10, 565–574.
Priestley, C.H.B., Taylor, R.J., 1972. On the assessment of surface heat flux and evaporation using large-scale parameters. Mon. Weather Rev. 100, 81–92.
Ramírez, J.A., Hobbins, M.T., Brown, T.C., 2005. Observational evidence of the complementary relationship in regional evaporation lends strong support for Bouchet's hypothesis. Geophys. Res. Lett. 32, L15401, http://dx.doi.org/10.1029/2005GL023549.
Rayner, D.P., 2007. Wind Run Changes: the dominant factor affecting pan evaporation trends in Australia. J. Clim. 20, 3379–3394.

Roderick, M.L., Farquar, G.D., 2002. The cause of decreased pan evaporation over the past 50 years. Science 298, 1410–1411.
Roderick, M.L., Rotstayn, L.D., Farquhar, G.D., Hobbins, M.T., 2007. On the attribution of changing pan evaporation. Geophys. Res. Lett. 34, L17403, http://dx.doi.org/10.1029/2007GL031166.
Roderick, M.L., Hobbins, M.T., Farquhar, G.D., 2008a. Pan evaporation trends and the terrestrial water balance. I. Principles and observations. Geog. Compass, 746–760, http://dx.doi.org/10.1111/j. 1749-8198.2008.00213.x.
Roderick, M.L., Hobbins, M.T., Farquhar, G.D., 2008b. Pan evaporation trends and the terrestrial water balance. II. Energy balance and interpretation. Geog. Compass, 761–780, http://dx.doi.org/10.1111/j. 1749-8198.2008.00214.x.
Rotstayn, L.D., Roderick, M.L., Farquhar, G.D., 2006. A simple pan-evaporation model for analysis of climate simulations: evaluation over Australia. Geophys. Res. Lett., L027114, http://dx.doi.org/10.1029/2006GL027114.
Sabziparvar, A.A., Tabari, H.A.A., Ghafouri, M., 2010. Evaluation of class a pan coefficient modelsfor estimation of reference crop evapotranspiration in cold semi-arid and warm arid climates. Water Resour. Manage. 24, 909–920.
Shen, Y.J., Liu, C.M., Liu, M., Zeng, Y., Tian, C.Y., 2010. Change in pan evaporation over the past 50 years in the arid region of China. Hydrol. Process. 24, 225–231.
Stanhill, G., 2002. Is the class A evaporation pan still the most practical and accurate meteorological method for determining irrigation water requirements? Agric. Forest Meteorol. 112 (3–4), 233–236.
Sugita, M., Usui, J., Tamagawa, I., Kaihotsu, I., 2001. Complementary relationship with a convective boundary layer model to estimate regional evaporation. Water Resour. Res. 37, 353–365.
Szilagyi, J., Jozsa, J., 2008. New findings about the complementary relationship based evaporation estimation methods. J. Hydrol. 354, 171–186.
Szilagyi, J., 2001. On bouchet's complementary hypothesis. J. Hydrol. 246, 155–158.
Szilagyi, J., 2007. On the inherent asymmetric nature of the complementary relationship of evaporation. Geophys. Res. Lett., L028708, http://dx.doi.org/10.1029/2006GL028708.
Thom, A.S., Thony, J.L., Vauclin, M., 1981. On the proper employment of evaporation pans and atmometers in estimating potential transpiration. Q. J. R. Meteorol. Soc. 107, 711–736.
Twine, T.E., Kustas, W.P., Norman, J.M., Cook, D.R., Houser, P.R., 2000. Correcting eddy-covariance flux underestimates over a grassland. Agric. Forest Meteorol. 103, 279–300.
Willett, K.M., Jones, P.D., Gillett, N.P., Thorne, P.W., 2008. Recent Changes in surface humidity: development of the HadCRUH dataset. J. Clim. 21 (20), 5364–5383.
Yang, H.B., Yang, D.W., 2012. Climatic factors influencing changing pan evaporation across China from 1961 to 2001. J. Hydrol. 414–415, 184–193, http://dx.doi.org/10.1016/j.jhydrol.2011.10.043.
Yang, D.W., Sun, F.B., Liu, Z.Y., Cong, Z.D., Lei, Z.D., 2006. Interpreting the complementary relationship in non-humid environments based on the Budyko and Penman hypotheses. Geophys. Res. Lett. 33, L18402, http://dx.doi.org/10.1029/2006GL027657.
Zuo, H.C., Bao, Y., Zhang, C.J., Hu, Y.Q., 2006. An analytic and numerical study on thephysical meaning of pan evaporation and its trend in recent 40 years (in Chinese). Chin. J. Geophys. 49, 680–688.
Zuo, H.C., Li, D.L., Hu, Y.Q., Bao, Y., Lu, S.H., 2005. Characteristics of climatic trends and correlation between pan-evaporation and environmental factors in the last 40 years over China. Chin. Sci. Bull. 50, 1235–1241.